

Flexible CuS nanotubes–ITO film Schottky junction solar cells with enhanced light harvesting by using an Ag mirror

This article has been downloaded from IOPscience. Please scroll down to see the full text article.

2013 Nanotechnology 24 045402

(<http://iopscience.iop.org/0957-4484/24/4/045402>)

View [the table of contents for this issue](#), or go to the [journal homepage](#) for more

Download details:

IP Address: 42.244.4.227

The article was downloaded on 19/01/2013 at 02:43

Please note that [terms and conditions apply](#).

Flexible CuS nanotubes–ITO film Schottky junction solar cells with enhanced light harvesting by using an Ag mirror

Chunyan Wu¹, Zihan Zhang¹, Yiliang Wu¹, Peng Lv¹, Biao Nie¹, Linbao Luo¹, Li Wang¹, Jigang Hu¹ and Jiansheng Jie²

¹ School of Electronic Science and Applied Physics, Hefei University of Technology, Hefei Anhui 230009, People's Republic of China

² Institute of Functional Nano & Soft Materials (FUNSOM), Jiangsu Key Laboratory for Carbon-based Functional Materials and Devices, Soochow University, Suzhou Jiangsu 215123, People's Republic of China

E-mail: cywu@hfut.edu.cn and jsjie@suda.edu.cn

Received 7 October 2012, in final form 30 November 2012

Published 8 January 2013

Online at stacks.iop.org/Nano/24/045402

Abstract

Here we report the fabrication of a novel photovoltaic device based on CuS nanotubes (CuSNTs) and indium tin oxide (ITO) Schottky junctions. Large-quantity synthesis of CuSNTs was accomplished via a solution-based sacrificial template method under moderate conditions, while ITO Schottky contacts were fabricated via micro-fabrication and pulsed laser deposition (PLD). Upon light illumination, CuSNTs–ITO Schottky junctions exhibited pronounced photovoltaic behavior, giving rise to a power conversion efficiency of 1.17% on a conventional SiO₂/Si substrate. Furthermore, by utilizing PET as the substrate, transparent and flexible CuSNTs–ITO solar cells were constructed and showed performance close to their device counterparts on a rigid substrate. Notably, it was found that the flexible devices were robust against tensile strain and could stand a bending angle up to ~95°. To enhance the light absorption of the devices, an Ag mirror layer was deposited on the rear side of the PET substrate so as to allow multiple reflection and absorption of the incident light. As a result, the flexible devices showed a substantial performance improvement, yielding an efficiency of ~2%. Our results demonstrate that low-cost and environmentally friendly CuSNTs–ITO solar cells are promising candidates for new-generation photovoltaic devices.

 Online supplementary data available from stacks.iop.org/Nano/24/045402/mmedia

(Some figures may appear in colour only in the online journal)

1. Introduction

Utilization of clean and renewable energy sources, such as solar energy, has been greatly stimulated recently due to the limited reserves of carbon-based fuels, such as oil, natural gas, and coal, along with the environmentally damaging emissions associated with their combustion [1]. Conversion of solar energy to electricity by photovoltaic technologies represents

a rapidly growing component of the electricity market [2]. Solar devices based on various inorganic materials, such as monocrystalline and polycrystalline silicon, and thin films such as amorphous silicon (α -Si), Cu(In, Ga)Se_{2-x}S_x (CIGS), and cadmium telluride (CdTe), have already penetrated the market, owing to their broad spectral absorption, high carrier mobilities, and increased stability [3]. However, the high cost and relatively low throughput associated with

the vacuum-based techniques still hamper their further development. It remains a great challenge to fabricate low-cost marketable solar devices.

Copper sulfide (Cu_xS), an important p-type transition-metal chalcogenides semiconductor with abundant structures and components, including covellite CuS , anilite $\text{Cu}_{1.75}\text{S}$, digenite $\text{Cu}_{1.8}\text{S}$, djurleite $\text{Cu}_{1.95}\text{S}$, chalcocite Cu_2S and so on [4], has been widely used in diverse fields such as catalysts, nanoscale switches, thermoelectric and photoelectric transformers, and gas sensors [5–9]. The unique optoelectronic properties arising from the stoichiometry-dependent band-gap [10], for instance, 1.2 eV for Cu_2S , 1.5 eV for $\text{Cu}_{1.8}\text{S}$, and 2.2 eV for CuS , along with the fact that Cu_xS is an earth-abundant and environmentally benign solar absorption material, make Cu_xS a promising candidate for photovoltaic applications. In recent decades, thin-film photovoltaic cells composed of Cu_xS – CdS heterojunctions have emerged as a promising photovoltaic device for pilot plant production owing to their high powder conversion efficiency of more than 9.1%, easy fabrication, and low cost [11–14]. Recently, small-area Cu_2S – CdS solar cells with even higher efficiencies of 10% have been reported [15]. Nevertheless, the device fabrication process for the Cu_xS – CdS solar cells is very complicated; multi-step vacuum evaporation and surface treatments were involved. In addition, concern about the pollution resulting from the heavy metal ion Cd^{2+} in the CdS layer needs to be further solved.

It is well known that the junction formation as well as the surface treatment processes play important roles in determining the efficiency and stability of Cu_xS based solar cells [16]. Compared to the standard vacuum-based techniques, a solution-based process with straightforward comparative advantages of atmospheric pressure processing, suitability for large-area and flexible substrates, higher throughput, and the combination of more efficient materials usage and lower temperature processing, is expected to be an appealing alternative for solar cell construction. Also, the utilization of Cu_xS nanostructures with size- and morphology-dependent properties offers opportunities to greatly enhance the solar cell performance. For instance, heterojunction solar cells based on spin-cast Cu_2S and CdS nanocrystal layers through a low-temperature ($\leq 150^\circ\text{C}$) solution process showed improved performance and stability [17]. Very recently, Yang *et al* also reported the fabrication of photovoltaic cells based on CdS – Cu_2S core–shell nanowires (NWs) via a low-temperature solution-based cation exchange reaction, revealing an efficiency as high as 5.4% [18]. In addition, CdS – Cu_xS single nanorod heterojunctions in a lengthwise configuration topotaxially converted from hydrothermal-synthesized CdS nanorods also validated their potential advantages in solar cell applications [19]. However, the use of toxic Cd^{2+} ions and the questionable stability of the Cu_xS – CdS cell caused by Cu diffusion into the CdS segment adjacent to the interface may hamper their further development. Therefore, an effective and environmentally benign material that can pair well with Cu_xS is in great demand in order to create high-performance and low-cost photovoltaic devices.

Recently, we have successfully developed a low-temperature solution-based method for large-quantity synthesis of CuS nanostructures with various morphologies and structures, such as well-defined concave cuboctahedrons CuS crystals [20] and uniform CuS nanotubes (CuSNTs) [21]. Because of the hollow one-dimensional (1D) structure for efficient carrier separation and transportation [22, 23], CuSNTs show promise in high-performance solar cell applications. Herein, we report on the fabrication of Schottky-type solar cells based on CuSNTs using indium tin oxide (ITO), which is a widely used transparent electrode, as the Schottky contact. The light could easily pass through the transparent ITO layer and illuminate the junction, leading to a pronounced photovoltaic behavior of the CuSNTs –ITO Schottky devices. Furthermore, devices were fabricated on a flexible polyethylene terephthalate (PET) substrate as well as the rigid SiO_2/Si substrate. By taking advantage of a mirror reflection technique, an optimized conversion efficiency of $\sim 2\%$ was achieved. Owing to the simple device architecture and fabrication process as well as the use of nontoxic device materials and the capability for flexible devices, the CuSNTs –ITO Schottky junction solar cells show great potential for use in new-generation nano-photovoltaic devices.

2. Experimental details

CuSNTs with uniform geometry were synthesized in large quantity by a facile solution reaction at 80° for 12 h in ethylene glycol (EG) using Cu NWs as sacrificial templates and thiourea as the sulfur source, as reported elsewhere [21]. The resulting black solid products were collected by centrifuging the mixture, then washed with absolute ethanol several times and dried in vacuum at 60° for further characterization and device fabrication. As-synthesized products were characterized by x-ray diffraction (XRD, Rigaku D/Max-rB, $\text{Cu K}\alpha$ radiation, $\lambda = 1.54178 \text{ \AA}$), field-emission scanning electron microscopy (FESEM, Sirion 200 FEG), transmission electron microscopy (TEM, Hitachi H-800), and high-resolution transmission electron microscopy (HRTEM, JEOL-2010). Compositions of the products were detected by energy-dispersive x-ray spectroscopy (EDS, Oxford INCA, attached to SEM).

To assess the electrical properties of the CuSNTs , nanodevices based on CuSNTs for two-probe measurements were constructed. The as-synthesized CuSNTs were first dispersed onto the SiO_2 (300 nm)/ $\text{p}^+\text{-Si}$ substrates with the desired density. Then photolithography, e-beam evaporation, and a subsequent lift-off process were employed to define Au (50 nm) electrodes on the CuSNTs . In order to construct the CuSNTs –ITO Schottky junction solar cells, an ITO (150 nm) Schottky electrode was fabricated between the two adjacent Au electrodes through an additional photolithography process. Pulsed laser deposition (PLD with KrF excimer laser, Lambda Physik COMPexPro 102, 248 nm, 120 mJ, 5 Hz) was used to deposit the ITO film. Electrical characterization was performed on a semiconductor characterization system (Keithley 4200-SCS). White light

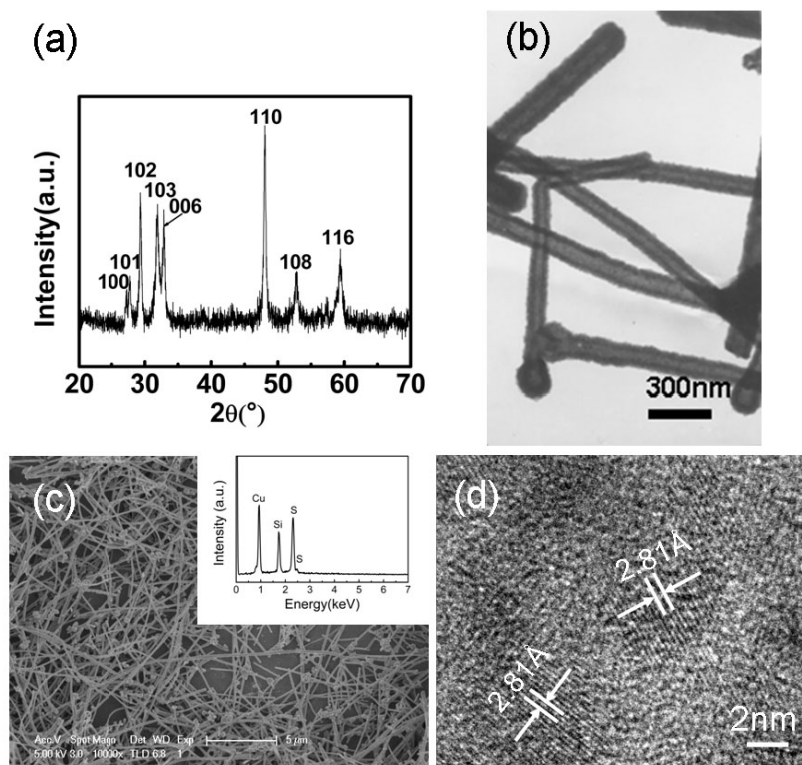


Figure 1. Structure and morphology characterizations of the CuSNTs. (a) XRD pattern, (b) TEM image, (c) FESEM image, and (d) HRTEM image of the as-prepared CuSNTs. Inset in (c) shows the corresponding EDS spectrum.

(3.5 mW cm^{-2}) from the optical microscopy on the probe station and a solar simulator (LE-SP-M300) with a calibrated illumination power density of 100 mW cm^{-2} were used as the light sources to detect the photovoltaic characteristics of the CuSNTs–ITO Schottky solar cells.

3. Results and discussions

Figure 1(a) depicts the XRD pattern of the as-prepared CuSNTs. All the diffraction peaks can be indexed as the pure hexagonal CuS phase (JCPDS card no. 6-464) and no evident peaks from impurities or other CuS phases are observed. TEM and FESEM investigations (figures 1(b) and (c)) clearly indicate that the products are straight NTs of 30–90 nm inner diameter and 20–50 nm wall thickness, with lengths up to tens of micrometer. The EDS spectrum in the inset of figure 1(c) reveals an atomic ratio of $\text{Cu}:\text{S} = 1:1.1$, which is close to the stoichiometric ratio of CuS. It is noted that the Si peak in the EDS spectrum comes from the Si substrate. In addition, the HRTEM image taken from the coarse outer wall of an NT demonstrates that the CuSNTs have polycrystalline structure. The lattice spacing of 2.81 \AA corresponds to the interplanar distance of (103) of hexagonal CuS (figure 1(d)).

Figure 2(a) shows the schematic illustration of the nanodevice for two-probe detection of the electrical characteristics of CuSNTs. Normally, there are about ten CuSNTs existing in the device channel region due to the large channel width. The number of CuSNTs in the channel will be taken into account in the following discussion and calculation.

The typical current versus voltage (I – V) curve between two Au electrodes in the dark is plotted in figure 2(b). The excellent Ohmic contact of the Au electrodes with the NTs is confirmed by the linear shape of the I – V curve. Notably, the conductivity deduced from the curve is as high as $\sim 1.6 \times 10^3 \text{ S cm}^{-1}$, indicating the highly conductive characteristic of the CuSNTs. It is noted that the cross-sectional area for the conduction channel was calculated by multiplying a single NT area by the number of NTs (~ 10) in the channel. To gain statistical significance, we have calculated the conductivity from 15 devices, and the corresponding histogram is shown in figure 2(c). The CuSNTs show a relatively narrow conductivity distribution of $\sim 8 \times 10^2$ – $5 \times 10^3 \text{ S cm}^{-1}$, which is of benefit to their device applications. However, the CuSNTs exhibit no visible change in the conductance upon light illumination or gate voltage (applied on the p^+ -Si substrate). This result might be due to the ultra-high conductivity of the CuSNTs; the hole concentration in the CuSNTs is so high that the light illumination and the gate voltage can hardly modulate the channel conductivity. For comparison, devices based on Cu NWs were also fabricated (supporting information, figure S1 available at stacks.iop.org/Nano/24/045402/mmedia). The conductivity of the Cu NWs is estimated to be $\sim 6.7 \times 10^5 \text{ S cm}^{-1}$, which is only about two orders of magnitude higher than that of the CuSNTs. These results clearly reveal that the CuSNTs possess extremely high conductivity with a semi-metal property.

The schematic illustration of the CuSNTs–ITO Schottky junction solar cell constructed on the SiO_2 (300 nm)/Si substrate is shown in figure 3(a). The ITO Schottky contact

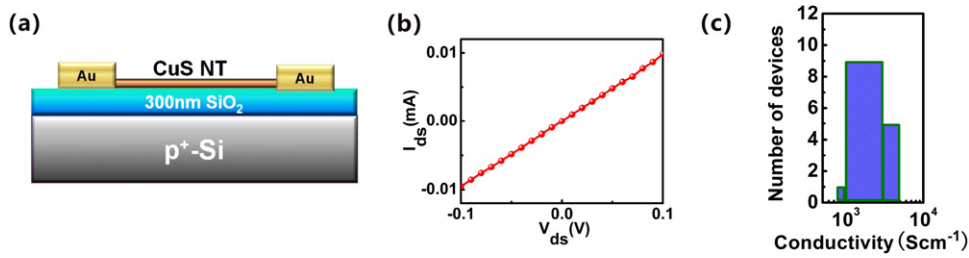


Figure 2. (a) Schematic illustration of the device for two-probe electrical measurement. (b) A typical I - V curve of the device in the dark. (c) Conductivity distribution of the CuSNTs deduced from 15 devices.

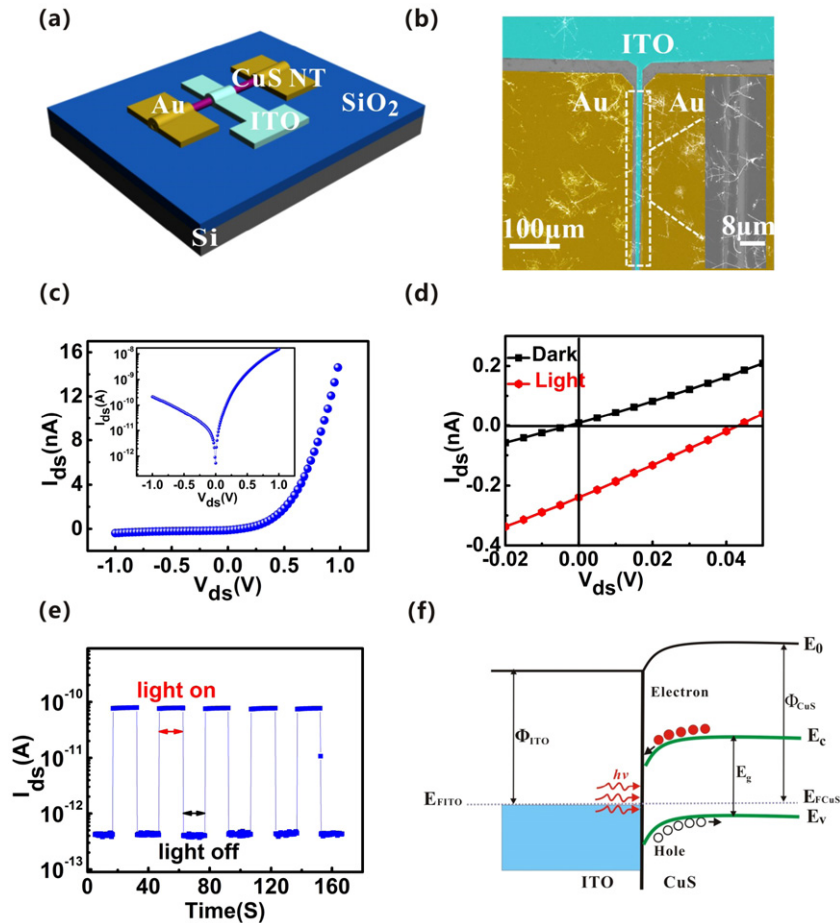


Figure 3. Photovoltaic characteristics of the CuSNTs–ITO Schottky junction solar cells fabricated on a SiO_2/Si substrate. (a) Schematic illustration of the device. (b) SEM image of a typical device with artificial colors. Inset displays the enlarged SEM image of the device channel. (c) Rectifying characteristics of the device in the dark. Inset shows the semi-logarithmic plot of the curve. (d) I - V curves of the device in the dark and under light illumination (white light, 3.5 mW cm^{-2}). (e) Photoresponse of the device at zero voltage bias. (f) Energy diagram of the CuSNTs–ITO Schottky junction under light illumination. Φ_{CuS} and Φ_{ITO} denote the work functions of the CuSNTs and the ITO, respectively. E_{FCuS} and E_{FITO} denote the Fermi energy levels of the CuSNTs and the ITO, respectively. E_{C} , E_{V} , and E_{g} represent the conduction band, valence band, and band-gap of the CuSNTs, respectively. E_0 is the vacuum energy level.

was fabricated between two adjacent Au Ohmic contacts. The I - V curve measured between the Au and ITO electrodes shows distinct rectifying characteristics with a turn-on voltage of $\sim 0.13 \text{ V}$ and a rectification ratio of $\sim 10^2$ (figure 3(c)). The ideality factor (n) could be deduced to be ~ 1.9 , based on the following equation:

$$n = \frac{q}{kT} \frac{dV}{d \ln I} \quad (1)$$

where q , k and T represent the electronic charge, Boltzmann's constant, and absolute temperature, respectively. This value is larger than that for an ideal diode ($n = 1$). This deviation is likely caused by the enhanced tunneling current in a nanoscale Schottky contact [24]. The ultra-high conductivity of the CuSNTs is also an important reason, since it can result in a large tunneling current. In spite of this, the device exhibits a pronounced photovoltaic behavior upon light illumination

(white light from the optical microscopy on the probe station, 3.5 mW cm^{-2}), as shown in figure 3(d). It is seen that the open circuit voltage (V_{oc}) and short circuit current (I_{sc}) are 45 mV and 265 pA, respectively. In addition, the fill factor (FF) and power conversion efficiency (η) could be deduced to be $\sim 22.4\%$ and $\sim 1.17\%$, respectively, according to the following equations:

$$FF = \frac{I_m V_m}{I_{sc} V_{oc}} \quad (2)$$

$$\eta = \frac{I_m V_m}{S P_{in}} \quad (3)$$

where I_m and V_m are the current and voltage at the maximum power output, respectively. S is the effective Schottky junction area ($\sim 6.5 \times 10^{-8} \text{ cm}^2$ for 10 CuSNTs in channel) and P_{in} is the incident power density. To study the effect of light intensity on the device performance, besides the white light with relatively lower intensity, the device characteristic was also examined under simulated light (AM 1.5 G) from a solar simulator (figure S2 available at stacks.iop.org/Nano/24/045402/mmedia). We note that V_{oc} , I_{sc} , and FF are further enhanced to 65 mV, 2.7 nA, 25.2%, respectively, while η decreases significantly to 0.68% under AM 1.5 G illumination. The decrease of η could be due to the different spectra of the light sources. The white light used in this study has a wavelength centered around 450 nm, while the solar spectra has a strong intensity in the range of 500–800 nm. Considering the relatively large band-gap of CuS (2.2 eV), the solar light could not be effectively absorbed. On the other hand, the large series resistance of the device as well as the severe interface recombination of the junction may also be responsible for the smaller η . It is suggested that the polycrystalline structure of the CuSNTs is an important factor that degrades the junction quality. Defects and grain boundaries in polycrystalline CuSNTs can serve as the recombination centers, resulting in a more rapid charge recombination at the junction interface compared with the monocrystalline nanostructure. We note that the open circuit voltage for the CuSNTs–ITO is relatively lower than the traditional Cu_2S –CdS p–n junction solar cells. This result could be ascribed to the ultra-high conductivity of the CuSNTs, as a result, the Schottky barrier height is reduced while the tunneling current is enhanced. Although materials and device optimization is demanded in future work to further improve the device performance, our results unambiguously reveal the potential of CuSNTs–ITO Schottky devices as low-cost and environmentally friendly solar cells.

To further investigate the working mechanism of the CuSNTs–ITO solar cells, the photoresponse characteristic of the device was measured, as shown in figure 3(e). The device shows high sensitivity to the incident light, with an I_{on}/I_{off} ratio $> 10^2$ and a fast response speed $< 0.3 \text{ s}$ at zero external bias, implying that the electron–hole pairs could be effectively generated and separated in the CuSNTs–ITO junction. Moreover, the device exhibits excellent reproducibility and stability under pulsed light illumination, indicating that the device can function as a high-performance photovoltaic-type photodetector operated at zero voltage bias. The energy

band diagram for the CuSNTs–ITO Schottky junction is illustrated in figure 3(f). The Schottky barrier due to the work function difference between the CuSNTs and ITO leads to the formation of a space–charge region. The built-in electric field has a direction from the ITO to the CuSNTs. When the junction is illuminated by incident light, electron–hole pairs will be excited by the photons with energy larger than the CuS band-gap. Subsequently, the photogenerated electron–hole pairs are separated at the space–charge region. The drift of the electrons and holes in opposite directions gives rise to the formation of the photocurrent.

New-generation solar cells require the devices be light weight and flexible as well [25–27]. In this work we further exploit the possibility of using CuSNTs–ITO solar cells in flexible nano-optoelectronics by using PET instead of the rigid SiO_2/Si as the device substrate. Figure 4(a) displays the schematic illustration of the device, and a photograph of the real device after bending is shown in figure 4(b). Notably, devices on the PET substrate have performances close to the device counterparts on the SiO_2/Si substrate. The representative device parameters are $V_{oc} = 60 \text{ mV}$, $I_{sc} = 157 \text{ pA}$, $FF = 25.8\%$, yielding a η value of 1.07% under the white light illumination (figure 4(c)). We note that I_{sc} is lower than that on the rigid substrate, which could be attributed to the worse electrical contact and consequently larger series resistance on the PET substrate. On the other hand, when the device is bent to a bending angle of 95° (defined as the corresponding central angle when the bent PET substrate was regarded as a circular arc of a whole circle, the width of the PET substrate was 2 cm), only a slight decrease in the performance is observed ($V_{oc} = 55 \text{ mV}$, $I_{sc} = 140 \text{ pA}$, $FF = 21.1\%$, and $\eta = 0.904\%$), indicating that the device is robust against tensile strain. Figure 4(d) plots the relationship of the power conversion efficiency with the bending angle from 0° (flat) to 110° . It is seen that the decline of the efficiency is not evident when the bending angle is small than 95° , but it decreases steeply from 0.904% at 95° to 0.23% at 110° . The decrease of efficiency at larger angles could be attributed to the degradation of the electrical contacts under large strain. Our results demonstrate that CuSNTs–ITO flexible devices can work well in a proper bending range, thus opening opportunities for new-generation nano-optoelectronic applications.

In the CuSNTs–ITO device, CuSNTs are lying on the substrate and the effective light absorption length is only equal to the NT diameter. As a result, most of the incident light will be lost and not absorbed by the device. This device structure differs from the vertically aligned NW arrays, which usually exhibit excellent light absorption due to the strong light trapping effect [28]. It seems that the inferior light absorption of the CuSNTs–ITO device is one of the key issues that limits its performance. To improve the device performance, here we developed a method called ‘mirror reflection’ to further enhance the light absorption of the CuSNTs–ITO device by depositing a layer of smooth Ag film (80 nm) on the rear side of the transparent PET substrate via e-beam evaporation. The smooth Ag film can serve as a highly reflective mirror to reflect the incident light back

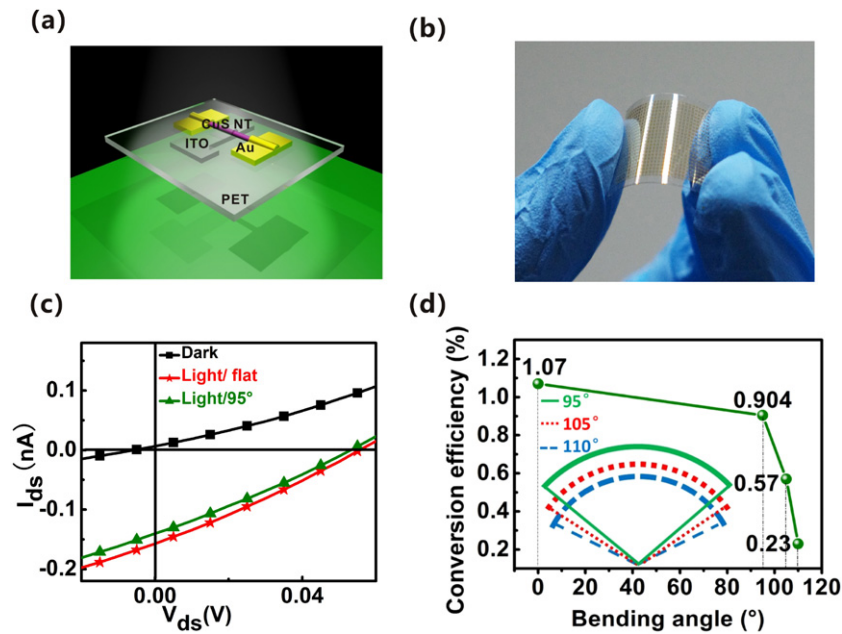


Figure 4. Photovoltaic characteristics of CuSNTs–ITO Schottky junction solar cells fabricated on a flexible PET substrate. (a) Schematic illustration and (b) photograph of the device. (c) Photovoltaic characteristics of the device measured when flat and at a bending angle of 95°. (d) Relationship of the power conversion efficiency with the bending angle.

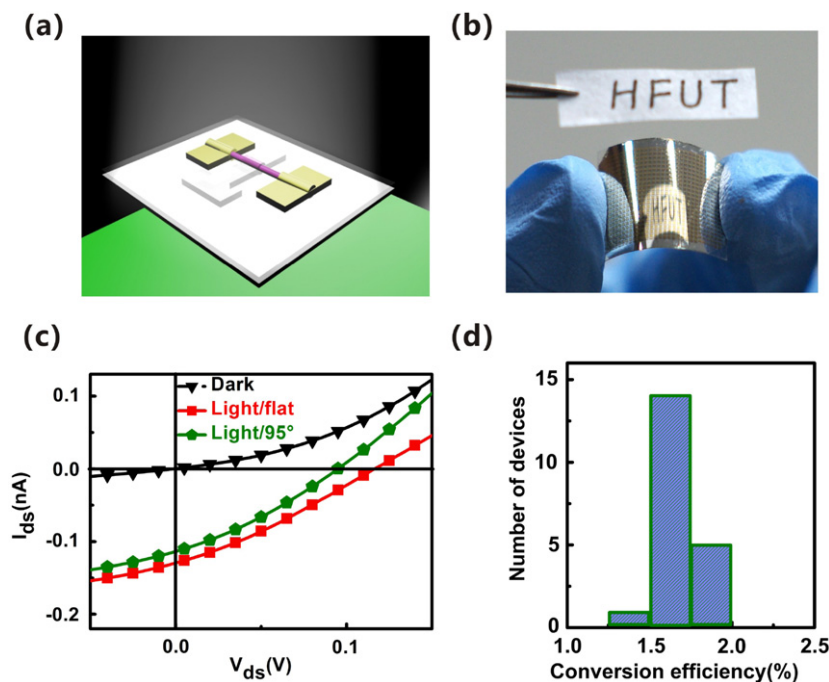


Figure 5. (a) Schematic illustration and (b) a photograph of the CuSNTs–ITO flexible solar cells with an Ag mirror layer on the rear side of the PET substrate. The logo of our university ‘HFUT’ could be reflected by the mirror. (c) Typical photovoltaic characteristics of the device with the Ag mirror measured when flat and at a bending angle of 95°, respectively. (d) Efficiency distribution for 20 devices used when flat.

to the device so that the light could be absorbed by the CuSNTs twice or even more times (figures 5(a) and (b)). Multiple reflection and absorption can lead to a substantial enhancement of the light absorption. Figure 5(c) shows the photovoltaic characteristics of the device detected when using the Ag mirror layer. Notably, V_{oc} , I_{sc} , and FF are improved to 120 mV, 132 pA and 28.2%, respectively, yielding a high η of 1.97% when the device is flat. A slight decrease in the

device performance is observed when the device was bent to a bending angle of 95° ($V_{oc} = 95$ mV, $I_{sc} = 117$ pA, FF = 29.82%, and $\eta = 1.46\%$). We note that the 25.9% decrease of η after bending is a little bit more than that for the device without an Ag mirror (15.5%). We presume that the reflection of the Ag mirror after bending is not as efficient as when flat. In this work, a total of 20 devices were measured, and their efficiency distribution when flat is shown

in figure 5(d). It is seen that the devices have efficiencies in the range 1.5–2.0%, which increase by at least a half compared to their device counterparts on PET without the Ag mirror layer. It is anticipated that the device performance could be further enhanced by controlling the CuSNT conductivity, improving the light absorption, and optimizing the device structure.

4. Conclusions

In summary, we conducted a systematic study on CuSNTs–ITO Schottky junctions and their potential applications in high-performance flexible photovoltaic devices. The junctions exhibited distinct rectifying characteristics in the dark. Further investigations under light illumination revealed the pronounced photovoltaic behavior of the devices, and a power conversion efficiency of $\sim 1.17\%$ was achieved on a SiO₂/Si substrate. Moreover, flexible solar cells based on CuSNTs–ITO junctions were constructed using PET as the substrate. It was found that the device performance could be maintained well under bending angles in the range 0°–95°, revealing the great potential of flexible CuSNTs–ITO junctions in new-generation and low-cost photovoltaic devices. To further improve the device performance, an Ag layer was deposited on the rear side of the PET substrate and served as a reflection mirror. The light absorption of the CuSNTs was greatly enhanced due to the multiple reflections and absorption of the incident light. As a result, the devices showed a remarkable improvement in the performance, giving rise to an efficiency of $\sim 2\%$. The low-cost fabrication of CuSNTs–ITO Schottky junction solar cells indicates a way towards fabricating solar cells based on Cu_xS nanostructures with environmentally friendly materials for future high-performance photovoltaic devices. Their tolerance to curvature also reveals their potential applications in hand-held consumer electronics as well as on convex roofs.

Acknowledgments

This work was supported by the National Key Basic Research Program of China (Nos 2012CB932400, 2010CB301802), the Major Research Plan of the National Natural Science Foundation of China (Nos 91233110, 91027021), the National Natural Science Foundation of China (NSFC, Nos 20901021, 51172151, 61106010, 21101051), and the Natural Science Foundation of Anhui Province of China (No. 11040606Q26).

References

- [1] Habas S E, Platt H A S, van Hest M F A M and Ginley D S 2010 *Chem. Rev.* **110** 6571
- [2] Report of the Basic Energy Sciences, *Workshop on Solar Energy Utilization 2005* available online at www.er.doe.gov/bes/reports/abstracts.html
- [3] Ginley D, Green M A and Collins R 2008 *MRS Bull.* **33** 355
- [4] Jiang X C, Xie Y, Lu J, He W, Zhu L Y and Qian Y T 2000 *J. Mater. Chem.* **10** 2193
- [5] Grozdanov I and Najdoski M 1995 *J. Solid State Chem.* **114** 469
- [6] Dachraoui M and Vedel J 1987 *Sol. Cells* **22** 187
- [7] Šetkus A, Galdikas A, Mironas A, Šimkiene I, Ancutiene I, Janickis V, Kaciulis S, Mattogno G and Ingo G M 2001 *Thin Solid Films* **391** 275
- [8] Sakamoto T, Sunamura H, Kawaura H, Hasegawa T, Nakayama T and Aono M 2003 *Appl. Phys. Lett.* **82** 3032
- [9] Chen X Y, Wang Z H, Wang X, Zhang R, Liu X Y, Lin W J and Qian Y T 2004 *J. Cryst. Growth* **263** 570
- [10] Yu J G, Zhang J and Liu S W 2010 *J. Phys. Chem. C* **114** 13642
- [11] Liu G M, Schulmeyer T, Brotz J, Klein A and Jaegermann W 2003 *Thin Solid Films* **431/432** 477
- [12] Rothwarf A and Barnett A M 1977 *IEEE Trans. Electron Devices* **24** 381
- [13] Gill W D and Bube R H 1970 *J. Appl. Phys.* **41** 3731
- [14] Rothwarf A 1980 *Sol. Cells* **2** 115
- [15] Bhat P K, Das S R, Pandya D K and Chopra K L 1979 *Sol. Energy Mater.* **1** 215
- [16] Pfisterer F 2003 *Thin Solid Films* **431/432** 470
- [17] Wu Y, Wadia C, Ma W L, Sadler B and Alivisatos A P 2008 *Nano Lett.* **8** 2551
- [18] Tang J Y, Huo Z Y, Brittman S, Gao H W and Yang P D 2011 *Nature Nanotechnol.* **6** 568
- [19] Mehta B R, Gupta S, Singh V N, Tripathi P and Varandani D 2011 *Nanotechnology* **22** 135701
- [20] Wu C Y, Yu S H and Antonietti M 2006 *Chem. Mater.* **18** 3599
- [21] Wu C Y, Yu S H, Chen S F, Liu G N and Liu B H 2006 *J. Mater. Chem.* **16** 3326
- [22] Yu Y Q et al 2011 *J. Mater. Chem.* **21** 12632
- [23] Li L, Wu P C, Fang X S, Zhai T Y, Dai L, Liao M Y, Koide Y, Wang H Q, Bando Y and Golberg D 2010 *Adv. Mater.* **22** 3161
- [24] Smit G D J, Rogge S and Klapwijk T M 2002 *Appl. Phys. Lett.* **81** 3852
- [25] McAlpine M C, Friedman R S and Lieber C M 2005 *Proc. IEEE* **93** 1357
- [26] McAlpine M C, Ahmad H, Wang D and Heath J R 2007 *Nature Mater.* **6** 379
- [27] Sun Y and Rogers J A 2007 *Adv. Mater.* **19** 1897
- [28] Xie C et al 2011 *Appl. Phys. Lett.* **99** 133113